International Journal of Digital Earth

ISSN: (Print) (Online) Journal homepage: https://www.tandfonline.com/loi/tjde20

Analyzing Antarctic ice sheet snowmelt with dynamic Big Earth Data

Dong Liang , Huadong Guo , Lu Zhang , Mingwei Wang , Lizhe Wang , Lei Liang & Zeeshan Shirazi

To cite this article: Dong Liang , Huadong Guo , Lu Zhang , Mingwei Wang , Lizhe Wang , Lei Liang & Zeeshan Shirazi (2020): Analyzing Antarctic ice sheet snowmelt with dynamic Big Earth Data, International Journal of Digital Earth, DOI: 10.1080/17538947.2020.1798522

To link to this article: https://doi.org/10.1080/17538947.2020.1798522

Published online: 30 Jul 2020.

INTERNATIONAL JOURNAL OF DIGITAL EARTH
https://doi.org/10.1080/17538947.2020.1798522

Analyzing Antarctic ice sheet snowmelt with dynamic Big Earth Data

Dong Liang [a,b], Huadong Guo[a,b], Lu Zhang[a,b], Mingwei Wang[c], Lizhe Wang[d], Lei Liang[a] and Zeeshan Shirazi[a]

[a]Key Laboratory of Digital Earth Science, Aerospace Information Research Institute, Chinese Academy of Sciences, Beijing, People's Republic of China; [b]University of Chinese Academy of Sciences, Chinese Academy of Sciences, Beijing, People's Republic of China; [c]Institute of Geological Survey, China University of Geosciences, Wuhan, People's Republic of China; [d]School of Computer Science, China University of Geosciences, Wuhan, People's Republic of China

ABSTRACT

Big Earth Data—big data associated with Earth sciences—can potentially revolutionize research on climate change, sustainable development, and other issues of global concern. For example, analyzing massive amounts of satellite imagery of polar environments, which are sensitive to the effects of climate change, provides insights into global climate trends. This study proposes a method to use Big Earth Data to explore changes in snowmelt over the Antarctic ice sheet from 1979 to 2016. The method uses Zernike moments to observe melt area in Antarctica and uses the Mann-Kendall test to detect temporal changes and abnormal information about the continent's melt area. The melting trend in the time-series data matched the changes in temperature and seasonal transitions. The results do not demonstrate significant change in the area of surface melt; however, abrupt changes in melt conditions linked to temperature changes over the Antarctic ice sheet were observed within the time series. The experiment results demonstrate that the proposed method is robust, adaptive, and capable of extracting the core features of melting snow.

ARTICLE HISTORY
Received 29 April 2020
Accepted 9 July 2020

KEYWORDS
Big Earth Data; data analysis; Antarctic ice sheet; Zernike moments; Mann-Kendall test

1. Introduction

In the past two decades, the capability to observe Earth and monitor its processes has been enhanced in terms of data quantity, quality, processing capability, and increasing accessibility to data and processing resources. This has given researchers insight into Earth like never before (Guo 2017a, 2017b). Remote, macro-level observations from satellite platforms over the past several decades have resulted in a vast repository of image data that is growing with evolving capabilities to generate petabytes of data within decreasing time frames. Effectively storing and efficiently retrieving data from increasingly structured databases enables analysis of this data in bulk, providing an opportunity to quantitatively map processes over longer time scales. The discipline of Earth science is quickly adapting to these developments and pooling multidisciplinary concepts and resources to evolve methods and platforms capable of maximizing the benefits of this growing technological potential. However, Earth observation data from both terrestrial and extra-terrestrial platforms require practices that are extremely multidisciplinary and innovative. This includes non-conventional uses of

CONTACT Lu Zhang zhanglu@radi.ac.cn; Mingwei Wang wmwscola@sina.com

digital data on human activity resulting from increasing interactions with technology. These practices can be collectively termed 'Big Earth Data' analysis (Guo et al. 2014; Guo, Wang, and Liang 2016). Simply put, Big Earth Data refers to big data associated with Earth sciences.

Similar to big data, Big Earth Data also derives methods and knowledge from traditional fields such as mathematics, statistics, computer science, remote sensing, geographic information systems (GIS), and the emerging fields of machine learning, data mining and artificial intelligence. These can be combined with domain-specific knowledge from Earth science; however, unlike traditional big data, Big Earth Data also has to deal with scale variances and the complexities of spatiotemporal data (Guo et al. 2020b). This is because Big Earth Data is characterized by multiple spatial and temporal scales as a consequence of multi-grade subsystems each with unique spatiotemporal characteristics, giving the acquired Earth observation data different rules and attributes at different scales (Guo et al. 2017).

Increasing global concern about climate change presents one of the most complicated challenges to the global community, and in particular for the Earth science community as they must not only understand the underlying global-scale processes but also support policy development towards mitigation. Within this context, polar regions showing evident and quantifiable effects from climate change over the years are of particular interest, as polar ice sheets are sensitive indicators of climate change. The changes within these polar environments are concerning as the melting of ice sheets in these regions will result in rising sea levels, creating problems for coastal settlements throughout the world (Lenaerts et al. 2019). Collectively, the Antarctic and Greenland ice sheets contain more than two thirds of the planet's freshwater (IPCC 2014a). Complete disintegration of only the Antarctic ice sheet would raise the level of the oceans by more than 58 m, inundating many of the world's major human settlements (Fretwell et al. 2013; Shepherd et al. 2018). The Intergovernmental Panel on Climate Change (IPCC) Fifth Assessment Report (IPCC 2014b) and the IPCC special report on the impacts of global warming of 1.5°C cite several studies that suggest nearly complete melting of polar ice sheets will occur at thresholds as low as 1°C and as high as 4°C of warming (IPCC 2018). The future of these ice sheets is therefore a challenging and complicated environmental policy issue for the coming years. This issue has also become relevant to efforts towards sustainability within the context of the United Nations' Sustainable Development Goals (SDGs) (United Nations 2015) and beyond. Understanding the mechanisms of these changes and identifying anthropogenic impacts will help to define success in achieving true sustainability (Guo 2019a, 2019b, 2020). Big Earth Data analysis and innovative uses of data and technology have the potential to provide novel solutions to understand climate change and facilitate mitigation processes (Guo, Goodchild, and Annoni 2020a; Guo, Fu, and Liu 2019).

Estimating ice sheet mass balance is a critical step in providing the necessary evidence of ongoing changes and understanding likely future scenarios. The surface mass balance, one of the two components of the ice sheet mass balance, is defined by the difference in influx of mass, e.g. precipitation, and outflux (runoff, evaporation or sublimation, snow erosion, etc.). Runoff has an important component, snowmelt, occurring when temperatures rise above the melting point (0°C) for surface snow (Lenaerts et al. 2019). In Antarctica, the average melt duration in a year is about one month and the duration for 80% of the melt area is less than 10 days. Moreover, the melt area is limited to 10% of the total Antarctic ice sheet area (Liang, Li, and Zheng 2019). Therefore, its direct impact on the ice sheet mass balance is negligible; however, snowmelt over the surface can significantly affect the albedo characteristics of the surface ice, as wet snow absorbs more radiation compared to dry snow and can result in significant indirect effects on the ice sheet mass balance (Zheng et al. 2018). Snowmelt can also have several other indirect implications, such as formation of supraglacial lakes on the surface (Stokes et al. 2019), or it may percolate into the ice, leading to changes in ice sheet movement velocity or the ice shelf's rate of deterioration. It might also become a vapor source (Abdalati and Steffen 1997) for cloud formations, which has been found to enhance meltwater runoff on the Greenland ice sheet (Van Tricht et al. 2016). Therefore, snowmelt is an important component to be quantified when evaluating ice sheet mass balance.

Earth observing satellites provide an ideal vantage point for collecting macro-level observations to monitor and assess snowmelt dynamics in vast areas such as the Antarctic ice sheet. Within the electromagnetic spectrum, the microwave spectrum is sensitive to large changes in the dielectric constant resulting from the melting of the ice sheet, providing advantages in applications of microwave remote sensing to monitor snowmelt phenomena over large areas (Hanna et al. 2013). Passive microwave brightness temperature is known to be sensitive to changes in snowfall, snow age, snowmelt, snow density and densification (Zwally and Gloersen 1977; Ulaby, Moore, and Fung 1986), and unlike the visible and infrared spectrum, microwave wavelengths allow monitoring even in cloudy conditions (Haggerty and Curry 2001; Lee and Sohn 2015; Skofronick-Jackson, Gasiewski, and Wang 2002). Currently, the acquisition of melt-area information on the surface of the ice sheet mainly depends on data from microwave radiometers and scatterometers (Liang, Li, and Zheng 2019). Understandably, various methods for detecting ice sheet melt have been developed and implemented utilizing passive microwave datasets. Snowmelt information on the Antarctic ice sheet has been recorded in various datasets, such as annual melt onset, end dates, and duration on the Antarctic Peninsula (Bevan et al. 2018); snowmelt observations using microwave remote sensing (Picard and Fily 2006); and snowmelt data for the whole of Antarctica (Liang, Li, and Zheng 2019). About 40 years of snowmelt information for the Antarctic ice sheet has been obtained.

In recent years, a popular topic in Antarctic ice sheet research has been the use of rich, large-scale, long-term snowmelt information to better discover and understand spatiotemporal phenomena and their relationship to environmental changes. Several advanced methods have been utilized to analyze the change in Antarctic ice sheet snowmelt over time-series data, such as wavelet transforms and neural networks (Liu, Wang, and Jezek 2005; Tedesco et al. 2004; Wang et al. 2018). These methods consider the changes in melt areas and changes in time but ignore the relationship between them. Zernike moments have been widely used to detect the change in pixel distribution on an amount of images (Wang and Healey 1998) and the Mann-Kendall test has been utilized to find abrupt changes in time-series data (Chen et al. 2016). These two techniques can be combined to analyze the spatial changes in melt area and temporal changes in melting phenomena (Fan and Tjahjadi 2017; Saadi et al. 2019).

This paper focuses on this issue in two ways. (1) Develop an efficient Big Earth Data analysis method based on Zernike moments and Mann-Kendall test techniques to detect changes in fixed areas over a time series and identify abrupt changes in large data volumes focusing on surface melt over the Antarctic ice sheet. Then, (2) investigate and analyze the trends and changes in snowmelt over the Antarctic ice sheet. The paper is outlined as follows. Datasets are listed in Section 2, the data analysis methodology is provided in Section 3, Section 4 presents the results, a discussion is given in Section 5, and Section 6 presents the conclusions.

2. Antarctic ice sheet and data

2.1. Study area

Antarctica is located at Earth's southernmost point and consists of ice shelves and islands in addition to the continent itself. The total area is 14.051 million km^2, which accounts for 9.4% of Earth's land area, while 98% of the Antarctic continent is covered by snow and ice throughout the year, with an average thickness of 2000–2500 m and a maximum thickness of 4200 m. The Antarctic ice sheet is generally divided into three parts, the East Antarctic and West Antarctic ice sheets and parts of the Antarctic Peninsula ice sheet (Golledge et al. 2019). The West Antarctic ice sheet is a fold belt composed of mountains, plateaus, and basins. The area of the East Antarctic ice sheet is twice the area of the West Antarctic ice sheet. Antarctica has a cold, dry, mostly continental climate, though the Antarctic Peninsula has a relatively mild

climate. Interannually cyclic freezing and thawing of the Antarctic ice sheet occurs mainly in areas near the coastal zone and on ice shelves.

2.2. Data

The dataset used in this study was developed using the brightness temperature data from passive microwave sensors including the Scanning Multichannel Microwave Radiometer (SMMR), the Special Sensor Microwave/Imager (SSM/I), and the Special Sensor Microwave Imager Sounder (SSMIS) from the Nimbus 7, DMSP (F8, F11, F13) and DMSP-F17 satellites, respectively. The remote sensing inversion method used for microwave radiometers is an improved wavelet transform-based algorithm for detecting ice sheet melt. It uses a sophisticated sampling scheme and a generalized Gaussian adaptive optimal threshold algorithm to obtain a more accurate classification threshold for dry and wet snow over the Antarctic ice sheet (Liu, Wang, and Jezek 2005; Liang, Li, and Zheng 2019).

The dataset consists of snowmelt information, such as annual melt onset, end dates, and duration at a spatial resolution of 25 km from 1979 to 2016. The blue area in Figure 1 shows the areas that experienced snow melt from 1979 to 2016, excluding 1987. Figure 2 is a compilation of annual snowmelt durations for each year in the study period. The detection accuracy of the dataset is reported to be higher than 70% when validated using Antarctica's automated weather station data. This dataset marks the starting point of the year as July 1st and the end of the year as June 30th of the following year. Therefore, the label '1979' for the first image in Figure 2 refers to the snowmelt information between 1 July 1979 to 30 June 1980, and the same nomenclature has been followed for the rest of the images. The Antarctic snowmelt data was downloaded from an online data sharing platform, the Chinese Academy of Sciences Strategic Priority Research Program of the Big Earth Data Science Engineering Program (CASEarth) (http://data.casearth.cn/sdo/detail/5c19a5690600cf2a3c557b90). The land mask of Antarctica was acquired from the National Snow and Ice Data Center (https://nsidc.org/data/polar-stereo/tools_mask.html).

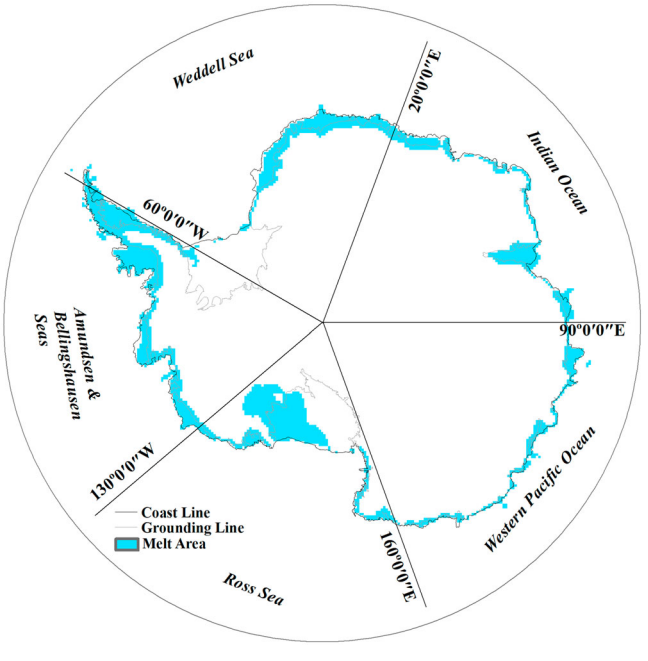

Figure 1. Accumulated extent of melt area from 1979 to 2016 (excluding 1987) in Antarctica obtained from the daily melting dataset.

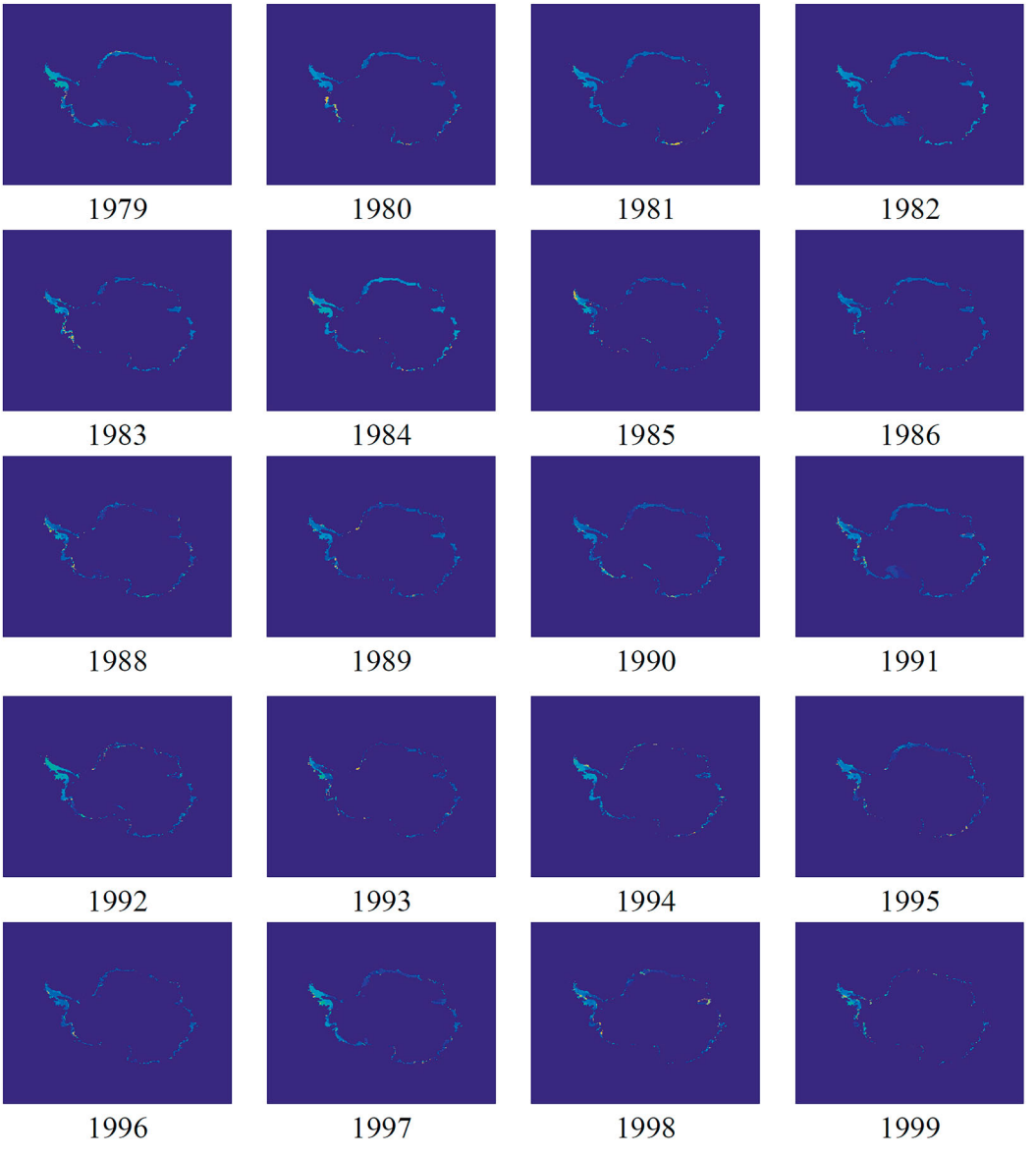

Figure 2. Images of snowmelt durations from 1979 to 2016 (excluding 1987).

3. Methods

3.1. Overall workflow of ice sheet snowmelt change analysis

Figure 3(a) and (b) show the flowchart and pseudocode for the overall workflow of the ice sheet snowmelt change analysis in this paper. The Zernike moment chooses the variables to express the scale and orientation invariant characteristics that were utilized to analyze the general change in melt area and obtain the special transformation features for each year. In Figure 2, the distribution of melt area consists of a series of discrete points approximated to circle characteristics with small intervals, which is suitable for the application of the Zernike moment technique. Then the changes were compared with those in the subsequent year by the feature value on different scales. A small value means the melt area did not obviously change over time.

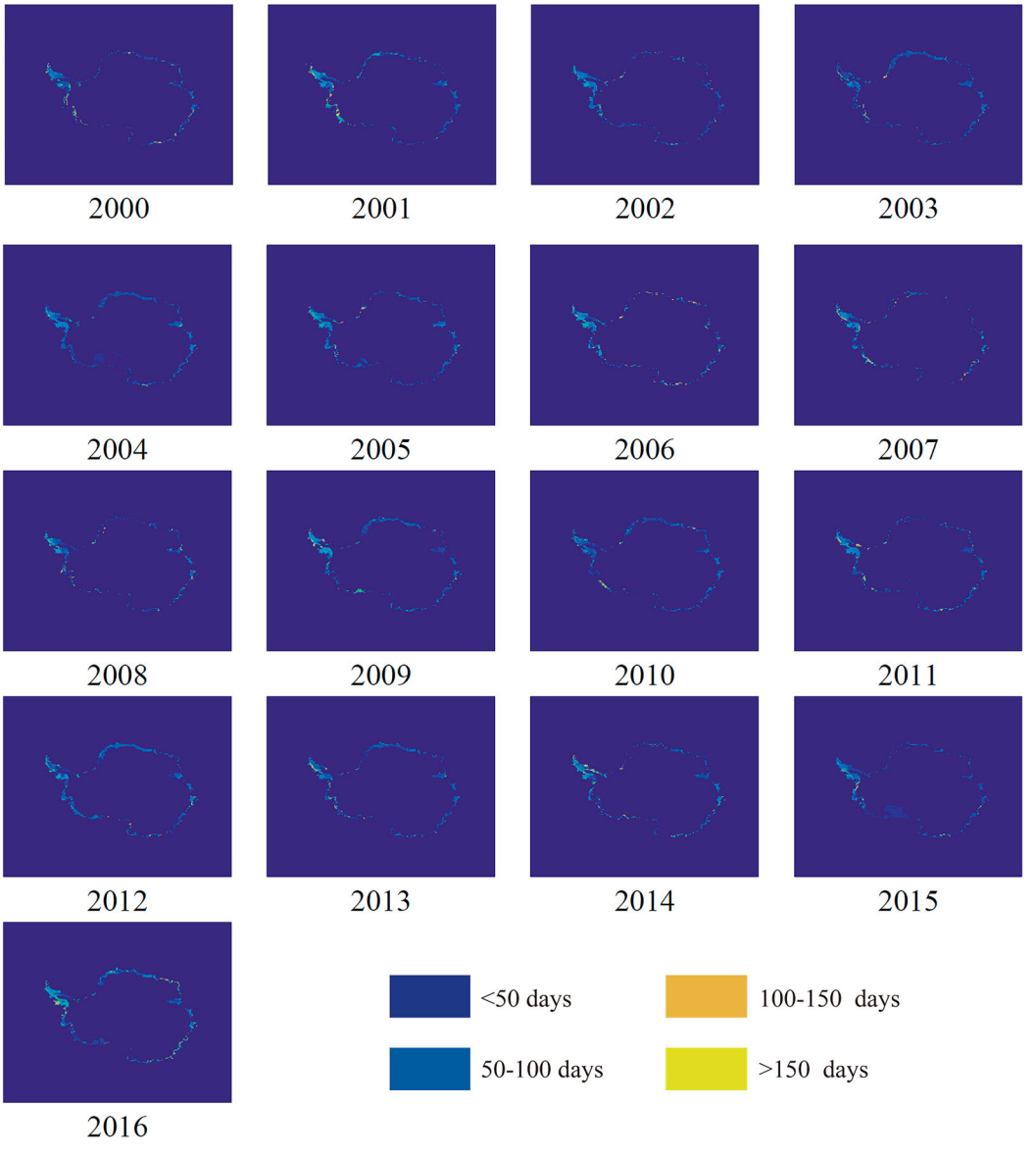

Figure 2 *Continued*

Afterwards, the Mann-Kendall test was used to detect changes and abnormalities in the monthly time series for December, January, February, and March, which constitute the summer season for the Antarctic ice sheet. For the Mann-Kendall test, the points of intersection between the UB and UF statistical curves indicate the year of abrupt change in melting when plotted with years on the horizontal axis (Figure 6). The main process of the proposed spatiotemporal snowmelt analysis method over the Antarctic is demonstrated as follows.

3.2. Zernike moments

Zernike moments were introduced by Teague to overcome the shortcomings of information redundancy present in geometric moments. Zernike moments represent the properties of an image with no redundancy or overlap of information between the moments (Khare, Srivastava, and Khare 2017).

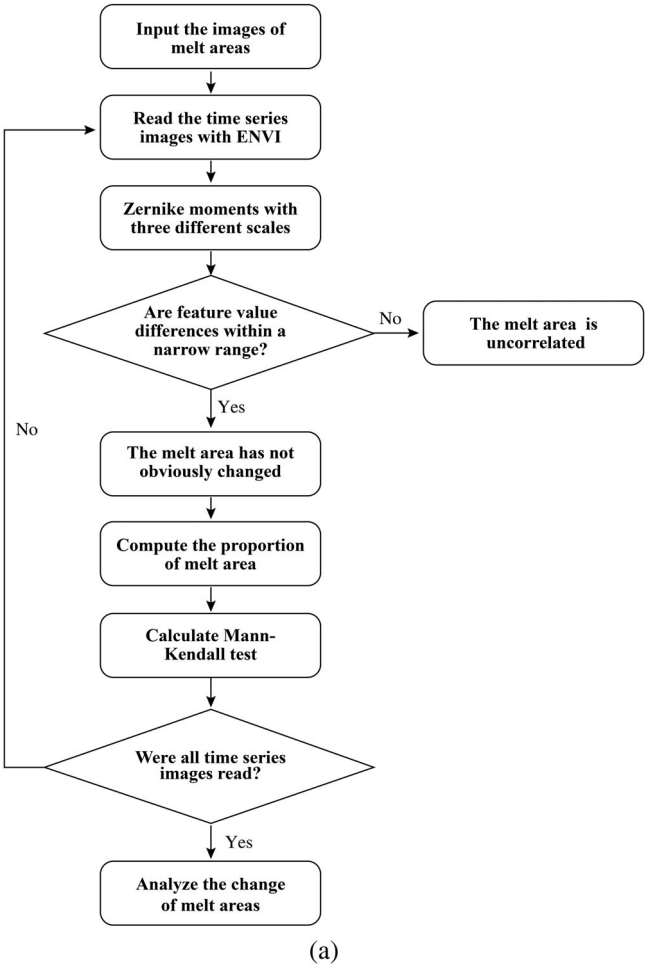

Figure 3. The flowchart (a) and pseudocode (b) for the overall workflow of the ice sheet snowmelt change analysis.

Due to these characteristics, Zernike moments can be utilized as feature sets to find the change in fixed areas over a time series.

Zernike moments have the following properties (Kaur, Pannu, and Malhi 2019; Kamal and Pachauri 2018):

(1) Zernike moments are rotation, translation, and scale invariant.
(2) Zernike moments are robust to noise and minor variations in shape.
(3) Since the basis of Zernike moments is orthogonal, they have minimal information redundancy.
(4) Zernike moments can characterize the global shape of a pattern. Lower-order moments represent the global shape pattern and higher-order moments represent the detail.
(5) An image can be better described by a small set of its Zernike moments than any other type of moment.

Zernike moments are a set of complex polynomials that form a complete orthogonal set over the interior of the unit circle of $x^2 + y^2 \leq 1$. These polynomials are of the form:

$$V_{mn}(x, y) = V_{mn}(r, \theta) = R_{mn}(r)e^{\,jn\theta} \tag{1}$$

where m is a positive integer and n is an integer subject to constraints $m - |n|$ and $|n| \leq m$; r is the length of the vector from the origin to pixel (x, y); θ is the angle between vector r and the x-axis in a

Algorithm: Spatiotemporal change detection of melt area based on the Zernike moments and Mann-Kendall test

Input: The original melt-area imagery dataset (1979 to 2016), and the number of images n=0.

Output: The proportion of melt area, feature values of Zernike moments on three scales, and UB and UF statistics of the Mann-Kendall test

1: Read the melt-area images using ENVI software, and transform them into a readable format;
2: **While** the images over the time series are not input completely
Do
3: n = n+1
4: Implement Zernike moments with three different scales for the melt-area images of each year using Eq. (4);
5: Output the values of the transformation features of each image;
6: **If** the difference is within a slight range
7: The melt area has not obviously changed in different years;
8: **Else**
9: The melt area of the current year is unreasonable or uncorrelated;
10: **End if**
11: Compute the proportion of the melt area according to Fig. 2, and map the data to each month;
12: Calculate the statistical variables of the Mann-Kendall test using Eqs. (8)-(9);
13: **End while**
14: **Return** the spatiotemporal change in ice sheet features over the time series.

(b)

Figure 3 *Continued*

counterclockwise direction; and $R_{mn}(r)$ are the Zernike radial polynomials in (r, θ) polar coordinates defined as:

$$R_{mn}(r) = \sum_{s=0}^{(m-|n|)/2} \frac{(-1)^s (m-s)! r^{m-2s}}{s!\left(\frac{m+|n|}{2}-s\right)!\left(\frac{m-|n|}{2}-s\right)!} \tag{2}$$

The above-mentioned polynomial in Equation (2) is an orthogonal and satisfies the orthogonality principle. In addition, Zernike moments are the projection of image function $I(x, y)$ onto these orthogonal basis functions. The orthogonality condition simplifies the representation of the original image because generated moments are independent.

The Zernike moment of order m with repetition n for a continuous image function $I(x, y)$ that vanishes outside the unit circle is defined as:

$$Z_{mn} = \frac{m+1}{\pi} \iint_{x^2+y^2 \le 1} I(x, y)[V_{mn}(r, \theta)]dxdy \tag{3}$$

In the case of digital images, the integral is replaced by summation, given as:

$$Z_{mn} = \frac{m+1}{\pi} \sum_{x} \sum_{y} I(x, y)[V_{mn}(r, \theta)], \; x^2 + y^2 \leq 1 \tag{4}$$

3.3. Mann-Kendall test

The Mann-Kendall test is based on the correlation between the ranks of a time series and their time order, which can be utilized to search for abnormal information in the time series. For a time-series $X = \{x_1, x_2, \ldots, x_n\}$, the test statistic is given as:

$$S = \sum_{i<j} a_{ij} \tag{5}$$

where

$$a_{ij} = sign(x_j - x_i) = sign(R_j - R_i) = \begin{cases} 1 & x_i < x_j \\ 0 & x_i = x_j \\ -1 & x_i > x_j \end{cases} \tag{6}$$

R_i and R_j are the ranks of observations x_i and x_j of the time series, respectively. As can be seen from Equation (6), the test statistic depends only on the ranks of the observations, rather than their actual values, resulting in a distribution-free test statistic. This is true because if data were to be transformed to any distribution, the ranks of the observations would remain the same. Distribution-free tests have the advantage that their power and significance are not affected by the actual distribution of the data, unlike the regression coefficient test and other parametric trend tests, which assume normal distribution of data and are strongly affected by skewness in data.

Under the assumption that the data are independent and identically distributed, the mean and variance of the statistic in Equation (5) above are given as:

$$E(S) = 0 \tag{7}$$

$$V_0(S) = n(n-1)(2n+5)/18 \tag{8}$$

where n is the number of observations. The existence of tied ranks (equal observations) in the data results in a reduction of the variance of S to become:

$$V_0^*(S) = n(n-1)(2n+5)/18 - \sum_{j=1}^{m} t_j(t_j-1)(2t_j+5)/18 \tag{9}$$

where m is the number of groups of tied ranks, each with t_j tied observations.

Kendall also shows that the distribution of S tends toward normality as the number of observations becomes large. The significance of trends can be tested by comparing the standardized variable u with the standard normal variate at the desired significance level, where the subtraction or addition of unity in Equation (10) is a continuity correction (Hamed 2008).

$$u = \begin{cases} (S-1)/\sqrt{V_0(S)} & S > 0 \\ 0 & S = 0 \\ (S+1)/\sqrt{V_0(S)} & S < 0 \end{cases} \tag{10}$$

4. Results

4.1. Qualitative analysis of the melt area distribution

The annual surface melt images from 1979 to 2016 (Figure 2) were used to validate the relationship for each independent year using the positions of discrete points. Figure 4 gives the results of the Zernike moments at three scales, respectively defined as $m = 1$, $n = 1$, $m = 2$, $n = 0$, and $m = 2$, $n = 2$ for the melt area from 1979 to 2016.

In Figure 4, the images from 1979 to 2016 demonstrate the melt area characteristics of Antarctica, and values of the Zernike moments reflect the dynamic changes in shape of the melt area. The annual variance between the values of the Zernike moments is small for the three scales considered, which suggest that the melt areas were generally similar during each year of the study. Moreover, these results also suggest that pixel values in different input images have similar distribution without any obvious changes. For the small scale, set as $m = 1$, $n = 1$ in Equation (4), the values fluctuate between the range of 5 to 8, while the fluctuations are negligible for the higher scale, set as $m = 2$, $n = 2$ in Equation (4), varying between 0 and 1.2. This reveals that the distribution of discrete points is largely similar for the whole time series. These results strongly suggest that the melt area has not significantly changed between 1979 and 2016 in Antarctica.

4.2. Quantitative analyses of the melt area

To estimate the seasonal changes in snowmelt areas, the proportion of monthly surface melt was calculated from the CASEarth snowmelt data product. The pixels in the original snowmelt dataset range between 1 and 365, indicating the day of the melt. Using this information, the melting event was assigned the relevant month. After this the duration of melt was estimated for each pixel for each of the months. Figure 2 highlights the annually accumulated surface melt durations, with darker tones indicating fewer days detected to be in a melting state at the pixel's location. The monthly proportion of melting in the study area is shown in Figure 5, computed as:

$$P(i) = num(i)/(h*w) \tag{11}$$

where $num(i)$ is the number of pixels for the i-th month on the image, and h and w are respectively the height and width of the original images.

The Antarctic ice sheet surface is stable from June to November with the proportion of melting close to 0 (Figure 5). Significant melting is evident mainly from December to March, falling during the Antarctic summer, which usually begins in November and ends in March of the following year. Especially for December to March, the situation gradually begins in January, reaches the peak in February, and tends to thaw with the increase in temperature.

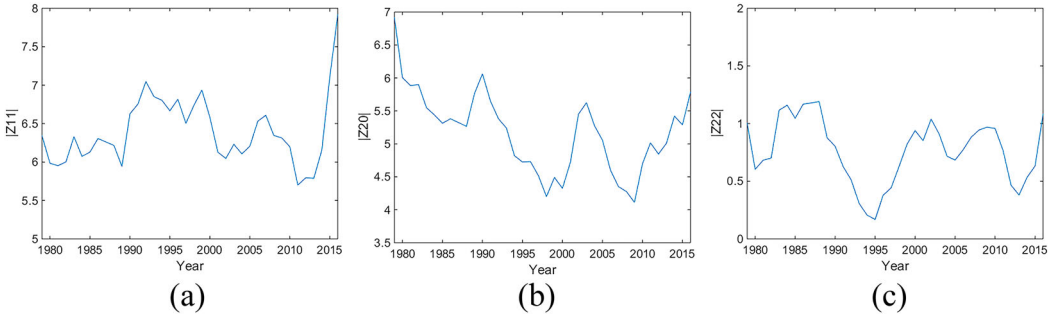

Figure 4. Results of the Zernike moments for spatial analysis of melt area in Antarctica at different scales: (a) $m = 1$, $n = 1$; (b) $m = 2$, $n = 0$; (c) $m = 2$, $n = 2$.

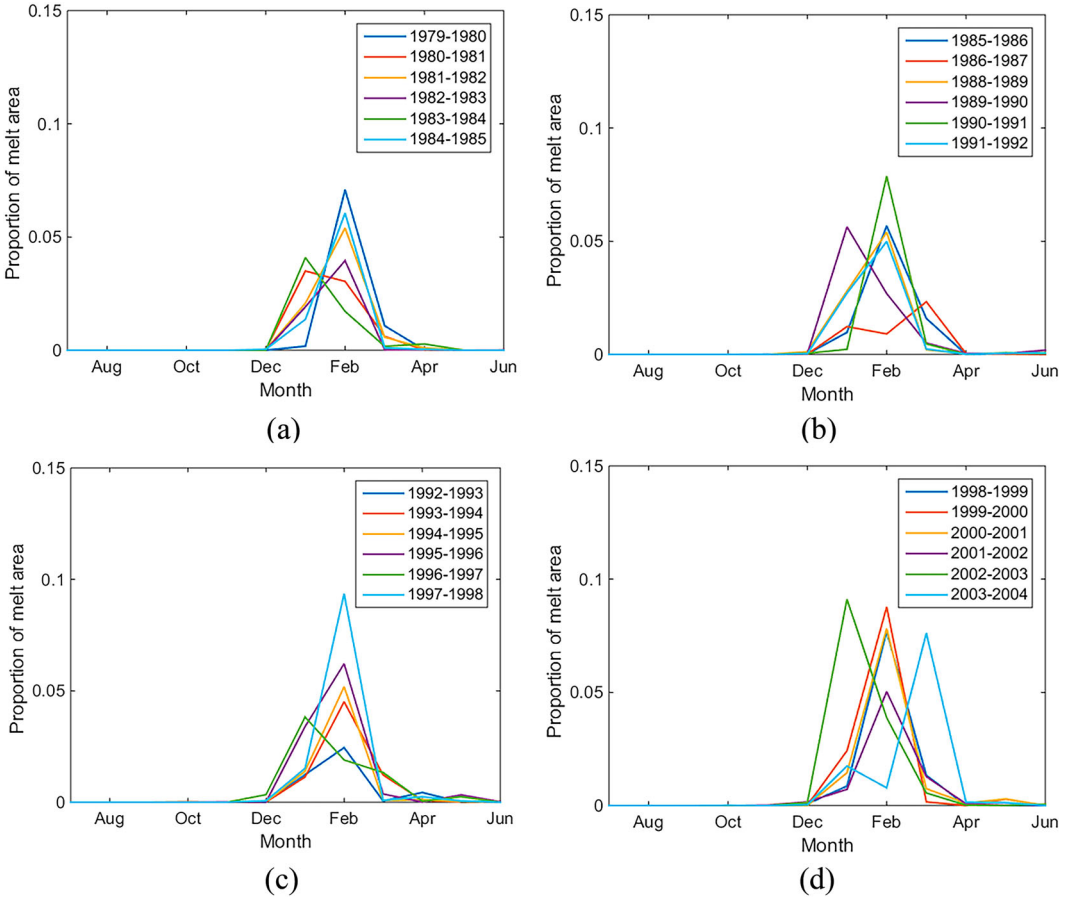

Figure 5. Proportion of melt area: (a) 1979–1984 (b) 1985–1991 (excluding 1987) (c) 1992–1997 (d) 1998–2003 (e) 2004–2009 (f) 2010–2016 (g) 1979–2016 (excluding 1987).

4.3. Quantitative analysis for abnormal melt detection

Since melting was mainly observed during December to March, data from these months was selected for quantitative analysis of abnormal melt detection. The melt area statistics from the same months were used with the Mann-Kendall test to calculate the UB and UF statistics for each year. The change curves of UB and UF statistics in selected months (December-March) are shown in Figure 6.

5. Discussion

This study attempted to understand the characteristics of surface snowmelt over the Antarctic by observing surface melt area and duration using Zernike moments and the Mann-Kendall test. In order to better understand the melting phenomenon, the mean of the annual average temperatures of several Antarctic stations (Amundsen Scott, Arturo Prat, Belgrano II, Bellingshausen, Casey, Dumont Durville, Faraday/Vernadsky, Gough, Great Wall, Halley, Macquarie, Marambio, Marion, Marsh, Mawson, McMurdo, Mirny, Neumayer, Novolazarevskaya, Orcadas, O'Higgins, Rothera, San Martin, Scott Base, Vostok, and Zhongshan) were calculated as shown in Figure 7. This information was obtained from the monthly station temperature data available on the British Antarctic Survey website (https://legacy.bas.ac.uk/met/READER/surface/stationpt.html). These stations had the minimum number of missing values.

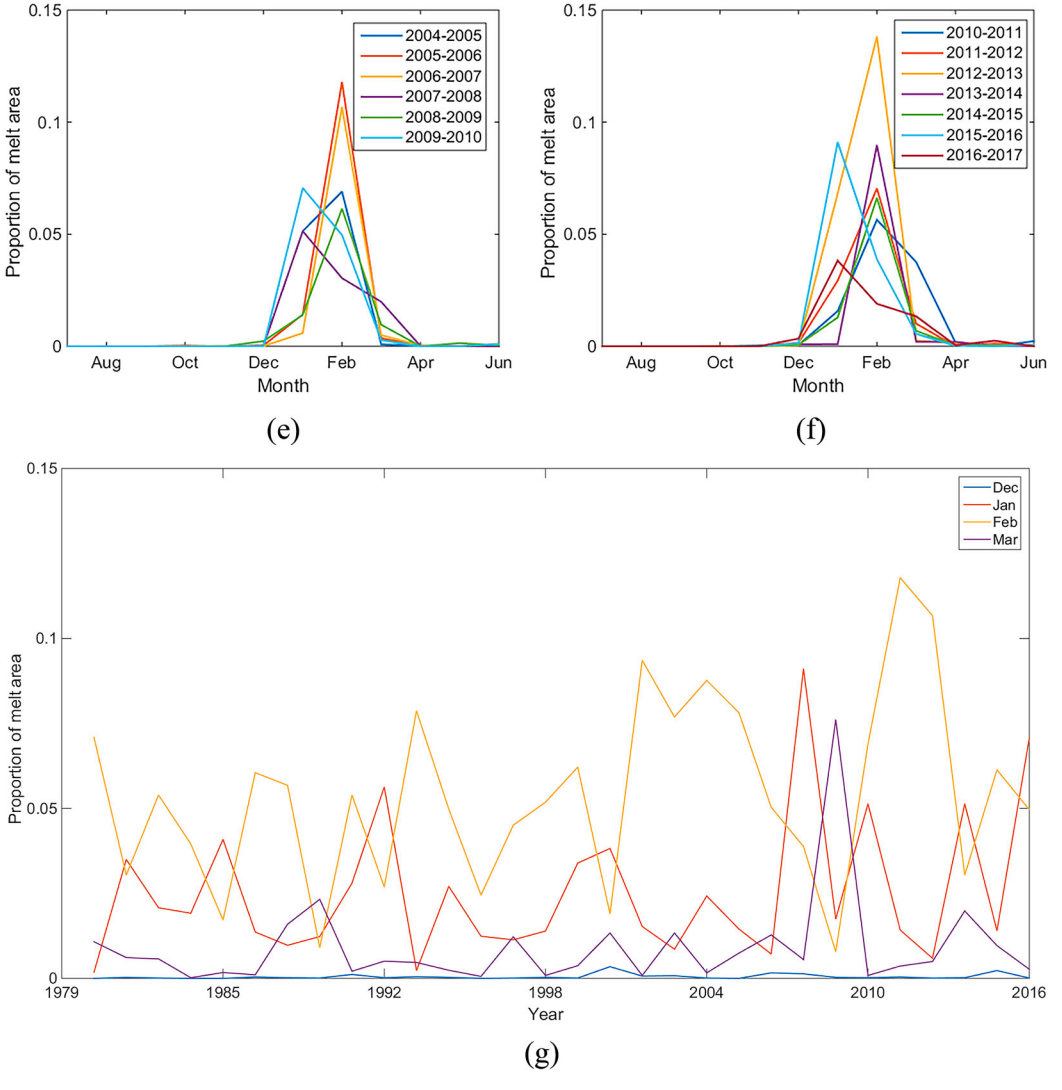

Figure 5 *Continued*

5.1. Spatiotemporal change analysis for snowmelt over the Antarctic

It is evident from the results that the melt area over Antarctica has not significantly changed in the past 40 years, which corresponds with observations suggesting insignificant changes in melt volume over the Antarctic (Kuipers Munneke et al. 2012). While it has been reported that there is a decreasing trend in the average annual melt area from 2002 to 2011 (Zheng et al. 2018), this might be due to the study consulting a relatively small time period. Looking at the spatial distribution of the melt activity in Figure 2, it can be concluded that consistent surface melt activity was concentrated along the coast of the Antarctic ice sheet and in particular over the Antarctic Peninsula. This has been reported to be increasing and has also been related to the Southern Hemisphere Annular Mode, linking melting over the peninsula to global atmospheric drivers (Barrand et al. 2013). Similarly, the snow melt durations in Figure 2 agree with the number of melt days in previous studies over the Antarctic ice sheet (Kuipers Munneke et al. 2012).

The results in Figure 5(f) had comparatively high surface melt area during January 2016, unlike in other years observed in this study. A strong melting event during the same time has been reported

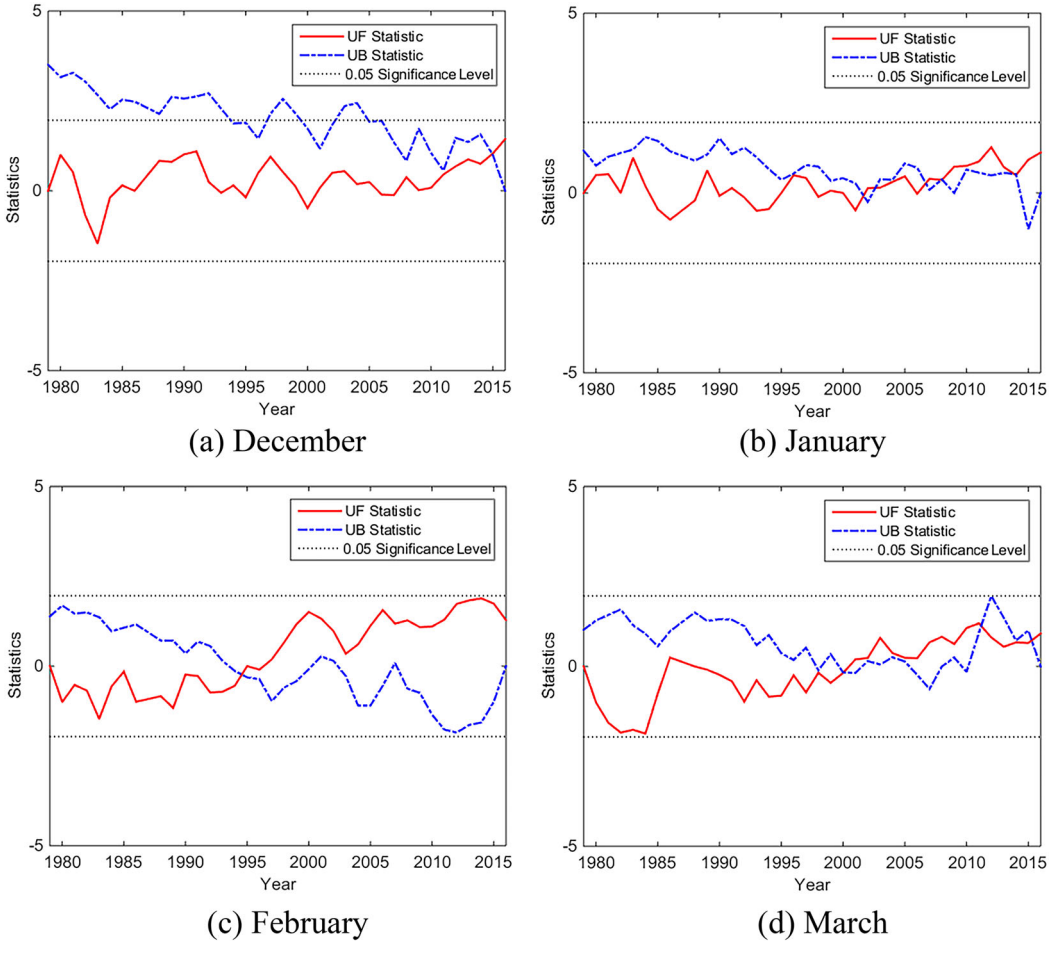

Figure 6. Change curves of UB and UF statistics: (a) December (b) January (c) February (d) March.

over the Ross Sea sector of the West Antarctic ice sheet (Nicolas et al. 2017), which also highlights a strong connection with the prevalent El Niño during the time period. Interestingly, a similar pattern can be observed for January in Figure 5(d) and (e) for the years 2003 and 2010, both of which had large melt areas, comparable to 2016, and moderate and strong El Niño conditions during those time periods, respectively. However, this relationship is not simple and the scale of melting and intensity of El Niño may not be directly related (Nicolas et al. 2017). Furthermore, this pattern is only observable for moderate or higher intensity El Niño events after 2000.

It has been established that surface melting on the Antarctic ice shelf is exponentially related to the near-surface summer air temperature (Trusel et al. 2015), which is also evident in this study as most of the melting is observed during the summer season. This observation is further strengthened when annual temperature extremes are considered, as they generally decrease from coastal areas towards central regions of Antarctica (Wei, Yan, and Ding 2019). The same surface melt pattern can be observed in these results.

5.2. Analysis of abnormal melt activity over the Antarctic

Figure 6 gives the UF and UB statistics for the summer months of December, January, February, and March, months with prominent surface melt activity. The UB and UF statistics exceeded the 0.05

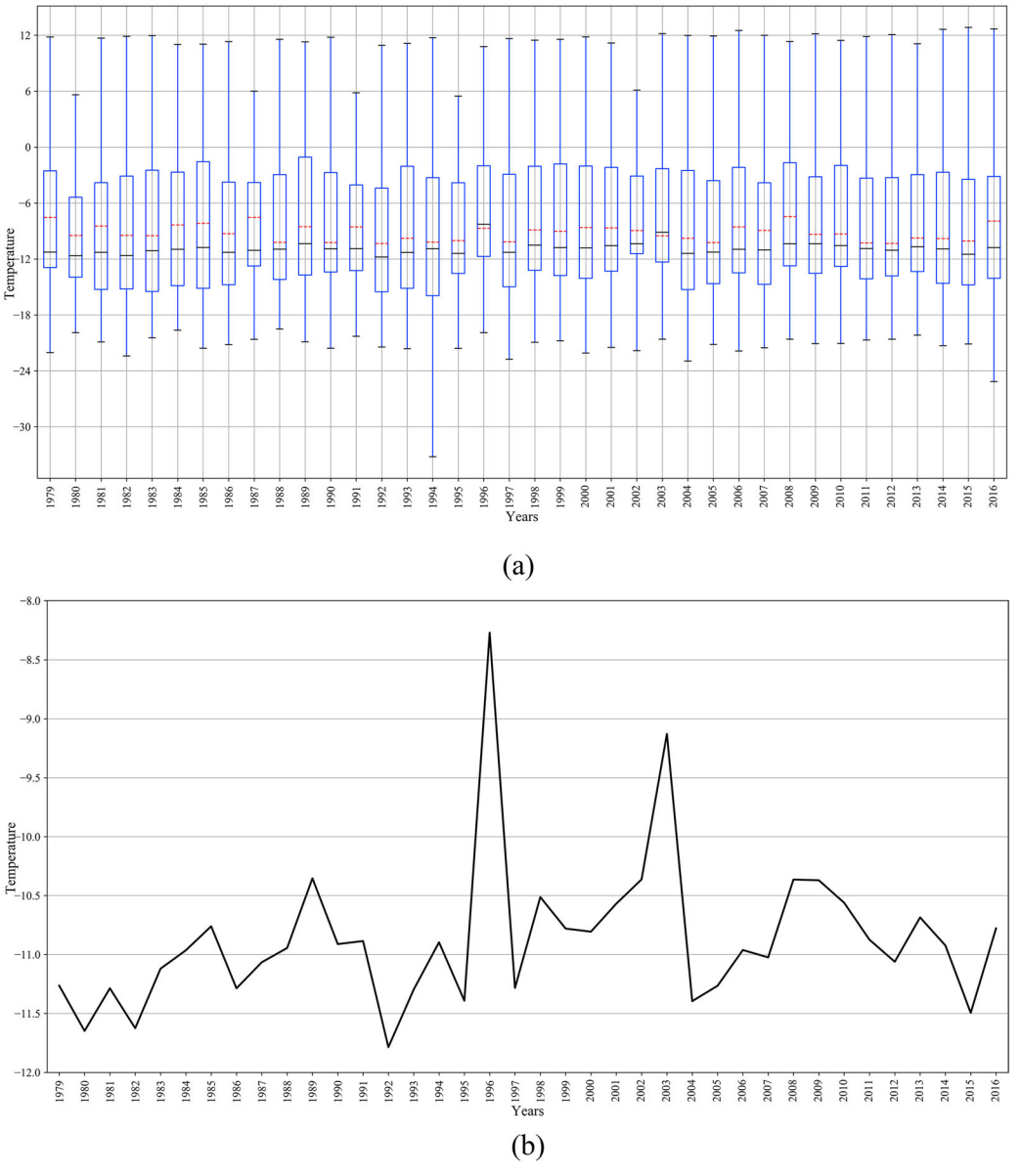

Figure 7. Temperature time series from 1979 to 2016. (a) Annual temperature variance for all selected weather stations in Antarctica with median values (red dashed lines) and mean values (black solid lines). (b) Annual temperature of Antarctica based on weather station records. (c) Temperature of Antarctica for selected months of December, January, February, and March.

confidence level in December, which suggests an extended melt duration. However, there were no obvious changes during January, February, and March. In addition, the intersection of the two lines signifies a sudden change in melt activity, and some of these changes can be related to temperature. From Figure 6, the months of February (c) and December (a) each had only one intersection in 1994 and 2015, respectively. Observing Figure 7(b), the annual temperature trend exhibited a steady gradual rise until 1994, after which the inter-annual temperature changes can be observed to be unstable, with increasing temperature differences between each year. Also, the year 1994 stands out in Figure 5(c) because large-scale melting was observed at both the beginning of the melting season in December and during the month of February. Before 1994, the melt area in December was

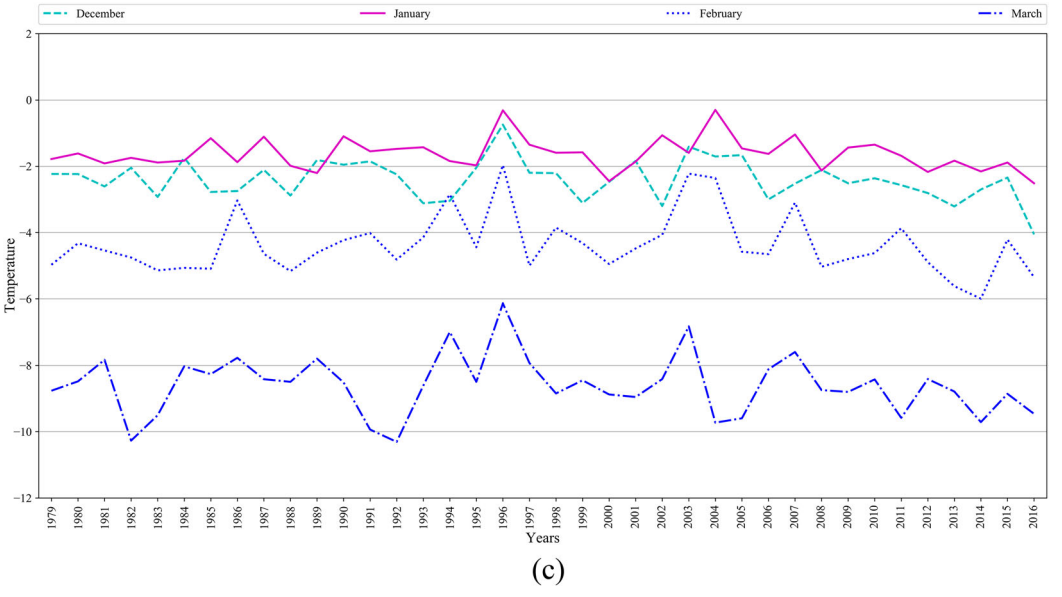

Figure 7 *Continued*

very small, but since 1994, melting has occurred repeatedly in December. In February, the range of melting after the 1994 season has increased significantly. The intersection in February can be related to a sudden drop in temperature (Figure 7(c)) after a net increase in temperature in the previous six years since 1988. For January, intersections can be observed in 1996, 2003, and 2008, the first two of which can be explained by a sharp increase in temperature in January of both 1996 and 2003. The intersection in March (Figure 6(d)) in 2000 and 2011 also indicates instability in the melting state of Antarctica, which has been observed to be intensifying in recent years. However, not all changes could be linked to temperature changes. Even though temperature has a strong influence on surface melt activity, there are other factors that have been observed to be linked to surface melting such as the SAM index (Barrand et al. 2013), foehn winds (van den Broeke 2005; Datta et al. 2019; Zou et al. 2019), and atmospheric rivers (Wille et al. 2019). Therefore, a more comprehensive cause and effect analysis is required for surface melting over the Antarctic ice sheet.

Within its scope, this study has demonstrated the usefulness of Zernike moments to analyze a large volume of data and the Mann-Kendall test to detect abrupt changes in melt area. The method performed well to detect changes in the melting state over Antarctica.

6. Conclusions

One of the important and challenging aspects of Big Earth Data analysis is to extract valuable information from a large volume of multi-source data. Computational resources, especially online cloud-based analysis platforms, provide feasible computation times. However, bandwidth limitations and limited connectivity in developing countries create challenging conditions to take advantage of Big Earth Data resources. This study demonstrates the usefulness of Zernike moments to analyze a large volume of data and the Mann-Kendall test to detect abrupt changes and provide a computationally inexpensive method to analyze Big Earth Data. This study used these techniques to observe the changes in melt area over the Antarctic ice sheet both in time and space between 1979 and 2016. Experiment results show that there was no obvious change in melt area at the three scales considered in the Zernike moment statistics between 1979 and 2016. The UB and UF statistics were observed to be on the boundary of the 0.05 level of significance from December to March each year, which proves

that the points of intersection between the UB and UF statistics indicate the years when there was an abrupt change in the melting state. Especially important, the study found that the year 1994 is the point in time when a different pattern emerged. The trends and sudden changes in the melting state obtained from analysis of different periods can be broadly explained when compared with temperature data from different stations in Antarctica.

In all, the proposed method performed well to analyze the change in melt area in Antarctica, which makes it more appropriate for practical applications. In the future, it will be interesting to collect more remote sensing data and conduct field surveys to analyze the cause of snowmelt in Antarctica. Understanding the mechanisms of change in the sensitive Antarctic environment can potentially provide insights about broader climate trends.

Acknowledgements

The authors are grateful for helpful comments from many researchers and colleagues, and we appreciate the feedback from the editor and anonymous referees.

Disclosure statement

No potential conflict of interest was reported by the author(s).

Funding

The research was supported by the Chinese Academy of Sciences Strategic Priority Research Program of the Big Earth Data Science Engineering Program (CASEarth) [grant numbers XDA19090000, XDA19030000] and National Natural Science Foundation of China [grant number 41876226].

ORCID

Dong Liang http://orcid.org/0000-0001-9147-7792

References

Abdalati, Waleed, and Konrad Steffen. 1997. "Snowmelt on the Greenland Ice Sheet as Derived From Passive Microwave Satellite Data." *Journal of Climate* 10 (2): 165–175. doi:10.1175/1520-0442(1997)010<0165:SOTGIS>2.0.CO;2.

Barrand, N. E., D. G. Vaughan, N. Steiner, M. Tedesco, P. Kuipers Munneke, M. R. van den Broeke, and J. S. Hosking. 2013. "Trends in Antarctic Peninsula Surface Melting Conditions From Observations and Regional Climate Modeling." *Journal of Geophysical Research: Earth Surface* 118 (1): 315–330. doi:10.1029/2012JF002559.

Bevan, Suzanne Louise, Adrian John Luckman, Peter Kuipers Munneke, Bryn Hubbard, Bernd Kulessa, and David William Ashmore. 2018. "Decline in Surface Melt Duration on Larsen C Ice Shelf Revealed by The Advanced Scatterometer (ASCAT)." *Earth and Space Science* 5 (10): 578–591. doi:10.1029/2018EA000421.

Chen, Yuzhuang, Yiqing Guan, Guangwen Shao, and Danrong Zhang. 2016. "Investigating Trends in Streamflow and Precipitation in Huangfuchuan Basin with Wavelet Analysis and the Mann-Kendall Test." *Water* 8: 3. doi:10.3390/w8030077.

Datta, Rajashree Tri, Marco Tedesco, Xavier Fettweis, Cecile Agosta, Stef Lhermitte, Jan T. M. Lenaerts, and Nander Wever. 2019. "The Effect of Foehn-Induced Surface Melt on Firn Evolution Over the Northeast Antarctic Peninsula." *Geophysical Research Letters* 46 (7): 3822–3831. doi:10.1029/2018GL080845.

Fan, Xijian, and Tardi Tjahjadi. 2017. "A Dynamic Framework Based on Local Zernike Moment and Motion History Image for Facial Expression Recognition." *Pattern Recognition* 64: 399–406. doi:10.1016/j.patcog.2016.12.002.

Fretwell, P., H. D. Pritchard, D. G. Vaughan, J. L. Bamber, N. E. Barrand, R. Bell, and C. Bianchi. 2013. "Bedmap2: Improved Ice Bed, Surface and Thickness Datasets for Antarctica." *The Cryosphere* 7 (1): 375–393. doi:10.5194/tc-7-375-2013.

Golledge, Nicholas R., Elizabeth D. Keller, Natalya Gomez, Kaitlin A. Naughten, Jorge Bernales, Luke D. Trusel, and Tamsin L. Edwards. 2019. "Global Environmental Consequences of Twenty-First-Century Ice-Sheet Melt." *Nature* 566 (7742): 65–72. doi:10.1038/s41586-019-0889-9.

Guo, Huadong. 2017a. "Big Data Drives the Development of Earth Science." *Big Earth Data* 1 (1–2): 1–3. doi:10.1080/20964471.2017.1405925.
Guo, Huadong. 2017b. "Big Earth Data: A New Frontier in Earth and Information Sciences." *Big Earth Data* 1 (1–2): 4–20. doi:10.1080/20964471.2017.1403062.
Guo, Huadong. 2019a. *Big Earth Data in Support of the Sustainable Development Goals (2019)*. Beijing: Science Press and EDP Sciences.
Guo, Huadong. 2019b. "From Digital Earth to Big Earth Data: Accelerating Scientific Discovery and Supporting Global Sustainable Development." *International Journal of Digital Earth* 12 (1): 1–1. doi:10.1080/17538947.2018.1559481.
Guo, Huadong. 2020. "Big Earth Data Facilitates Sustainable Development Goals." *Big Earth Data* 4 (1): 1–2. doi:10.1080/20964471.2020.1730568.
Guo, Huadong, Wenxue Fu, and Guang Liu. 2019. *Scientific Satellite and Moon-Based Earth Observation for Global Change*. Singapore: Springer. doi:10.1007/978-981-13-8031-0
Guo, Huadong, Michael F. Goodchild, and Alessandro Annoni. 2020a. *Manual of Digital Earth*. Singapore: Springer. doi:10.1007/978-981-32-9915-3
Guo, Huadong, Zhen Liu, Hao Jiang, Changlin Wang, Jie Liu, and Dong Liang. 2017. "Big Earth Data: A New Challenge and Opportunity for Digital Earth's Development." *International Journal of Digital Earth* 10 (1): 1–12. doi:10.1080/17538947.2016.1264490.
Guo, Huadong, Stefano Nativi, Dong Liang, Max Craglia, Lizhe Wang, Sven Schade, and Christina Corban. 2020b. "Big Earth Data Science: An Information Framework for a Sustainable Planet." *International Journal of Digital Earth* 13 (7): 743–767. doi:10.1080/17538947.2020.1743785.
Guo, Huadong, Lizhe Wang, Fang Chen, and Dong Liang. 2014. "Scientific Big Data and Digital Earth." *Chinese Science Bulletin* 59 (35): 5066–5073. doi:10.1007/s11434-014-0645-3.
Guo, Huadong, Lizhe Wang, and Dong Liang. 2016. "Big Earth Data From Space: A New Engine for Earth Science." *Science Bulletin* 61 (7): 505–513. doi:10.1007/s11434-016-1041-y.
Haggerty, Julie A., and Judith A. Curry. 2001. "Variability of Sea Ice Emissivity Estimated From Airborne Passive Microwave Measurements During FIRE SHEBA." *Journal of Geophysical Research: Atmospheres* 106 (D14): 15265–15277. doi:10.1029/2000JD900485.
Hamed, Khaled H. 2008. "Trend Detection in Hydrologic Data: The Mann–Kendall Trend Test Under the Scaling Hypothesis." *Journal of Hydrology* 349 (3): 350–363. doi:10.1016/j.jhydrol.2007.11.009.
Hanna, Edward, Francisco J. Navarro, Frank Pattyn, Catia M. Domingues, Xavier Fettweis, Erik R. Ivins, and Robert J. Nicholls. 2013. "Ice-Sheet Mass Balance and Climate Change." *Nature* 498 (7452): 51–59. doi:10.1038/nature12238.
Intergovernmental Panel on Climate Change. 2014a. "Summary for Policymakers." In *Climate Change 2013 – The Physical Science Basis: Working Group I Contribution to the Fifth Assessment Report of the Intergovernmental Panel on Climate Change*, 1–30. Cambridge: Cambridge University Press. doi:10.1017/CBO9781107415324.004
Intergovernmental Panel on Climate Change. 2014b. *Climate Change 2013 – The Physical Science Basis: Working Group I Contribution to the Fifth Assessment Report of the Intergovernmental Panel on Climate Change*. Cambridge: Cambridge University Press. doi:10.1017/CBO9781107415324
Intergovernmental Panel on Climate Change. 2018. *Global Warming of 1.5°C*. Geneva: World Meteorological Organization.
Kamal, Neel, and Sanjay Pachauri. 2018. "Mann-Kendall Test - A Novel Approach for Statistical Trend Analysis." *International Journal of Computer Trends and Technology* 63 (1): 18–21. doi:10.14445/22312803/IJCTT-V63P104.
Kaur, Parminder, Husanbir Singh Pannu, and Avleen Kaur Malhi. 2019. "Comprehensive Study of Continuous Orthogonal Moments – A Systematic Review." *ACM Computing Surveys* 52: 4. doi:10.1145/3331167.
Khare, Manish, Rajneesh Kumar Srivastava, and Ashish Khare. 2017. "Object Tracking Using Combination of Daubechies Complex Wavelet Transform and Zernike Moment." *Multimedia Tools and Applications* 76 (1): 1247–1290. doi:10.1007/s11042-015-3068-5.
Kuipers Munneke, P., G. Picard, M. R. van den Broeke, J. T. M. Lenaerts, and E. van Meijgaard. 2012. "Insignificant Change in Antarctic Snowmelt Volume Since 1979." *Geophysical Research Letters* 39: 1. doi:10.1029/2011GL050207.
Lee, Sang-Moo, and Byung-Ju Sohn. 2015. "Retrieving the Refractive Index, Emissivity, and Surface Temperature of Polar Sea Ice From 6.9 GHz Microwave Measurements: A Theoretical Development." *Journal of Geophysical Research: Atmospheres* 120 (6): 2293–2305. doi:10.1002/2014JD022481.
Lenaerts, Jan T. M., Brooke Medley, Michiel R. van den Broeke, and Bert Wouters. 2019. "Observing and Modeling Ice Sheet Surface Mass Balance." *Reviews of Geophysics* 57 (2): 376–420. doi:10.1029/2018RG000622.
Liang, Lei, Xinwu Li, and Fei Zheng. 2019. "Spatio-Temporal Analysis of Ice Sheet Snowmelt in Antarctica and Greenland Using Microwave Radiometer Data." *Remote Sensing* 11: 16. doi:10.3390/rs11161838.
Liu, Hongxing, Lei Wang, and Kenneth C. Jezek. 2005. "Wavelet-Transform Based Edge Detection Approach to Derivation of Snowmelt Onset, End and Duration From Satellite Passive Microwave Measurements." *International Journal of Remote Sensing* 26 (21): 4639–4660. doi:10.1080/01431160500213342.
Nicolas, Julien P., Andrew M. Vogelmann, Ryan C. Scott, Aaron B. Wilson, Maria P. Cadeddu, David H. Bromwich, and Johannes Verlinde. 2017. "January 2016 Extensive Summer Melt in West Antarctica Favoured by Strong El Niño." *Nature Communications* 8 (1): 15799. doi:10.1038/ncomms15799.

Picard, G., and M. Fily. 2006. "Surface Melting Observations in Antarctica by Microwave Radiometers: Correcting 26-Year Time Series From Changes in Acquisition Hours." *Remote Sensing of Environment* 104 (3): 325–336. doi:10.1016/j.rse.2006.05.010.

Saadi, Zulfaqar, Shamsuddin Shahid, Tarmizi Ismail, Eun-Sung Chung, and Xiao-Jun Wang. 2019. "Trends Analysis of Rainfall and Rainfall Extremes in Sarawak, Malaysia Using Modified Mann–Kendall Test." *Meteorology and Atmospheric Physics* 131 (3): 263–277. doi:10.1007/s00703-017-0564-3.

Shepherd, Andrew, Erik Ivins, Eric Rignot, Ben Smith, Michiel van den Broeke, Isabella Velicogna, and Pippa Whitehouse. 2018. "Mass Balance of the Antarctic Ice Sheet From 1992 to 2017." *Nature* 558 (7709): 219–222. doi:10.1038/s41586-018-0179-y.

Skofronick-Jackson, G. M., A. J. Gasiewski, and J. R. Wang. 2002. "Influence of Microphysical Cloud Parameterizations on Microwave Brightness Temperatures." *IEEE Transactions on Geoscience and Remote Sensing* 40 (1): 187–196. doi:10.1109/36.981360.

Stokes, Chris R., Jack E. Sanderson, Bertie W. J. Miles, Stewart S. R. Jamieson, and Amber A. Leeson. 2019. "Widespread Distribution of Supraglacial Lakes Around the Margin of the East Antarctic Ice Sheet." *Scientific Reports* 9 (1): 13823. doi:10.1038/s41598-019-50343-5.

Tedesco, M., J. Pulliainen, M. Takala, M. Hallikainen, and P. Pampaloni. 2004. "Artificial Neural Network-Based Techniques for the Retrieval of SWE and Snow Depth From SSM/I Data." *Remote Sensing of Environment* 90 (1): 76–85. doi:10.1016/j.rse.2003.12.002.

Trusel, Luke D., Karen E. Frey, Sarah B. Das, Kristopher B. Karnauskas, Peter Kuipers Munneke, Erik van Meijgaard, and Michiel R. van den Broeke. 2015. "Divergent Trajectories of Antarctic Surface Melt Under Two Twenty-First-Century Climate Scenarios." *Nature Geoscience* 8 (12): 927–932. doi:10.1038/ngeo2563.

Ulaby, Fawwaz T., Richard K. Moore, and Adrian K. Fung. 1986. *Microwave Remote Sensing Active and Passive-Volume III: From Theory to Applications*. Norwood, MA: Artech House, Inc.

United Nations. 2015. *Transforming Our World: The 2030 Agenda for Sustainable Development*. New York: United Nations.

van den Broeke, Michiel. 2005. "Strong Surface Melting Preceded Collapse of Antarctic Peninsula Ice Shelf." *Geophysical Research Letters* 32: 12. doi:10.1029/2005GL023247.

Van Tricht, K., S. Lhermitte, J. T. M. Lenaerts, I. V. Gorodetskaya, T. S. L'Ecuyer, B. Noël, M. R. van den Broeke, D. D. Turner, and N. P. M. van Lipzig. 2016. "Clouds Enhance Greenland Ice Sheet Meltwater Runoff." *Nature Communications* 7 (1): 10266. doi:10.1038/ncomms10266.

Wang, Lizhi, and G. Healey. 1998. "Using Zernike Moments for the Illumination and Geometry Invariant Classification of Multispectral Texture." *IEEE Transactions on Image Processing* 7 (2): 196–203. doi:10.1109/83.660996.

Wang, Xing-Dong, Xin-Wu Li, Cheng Wang, and Xin-Guang Li. 2018. "Antarctic Ice-Sheet Near-Surface Snowmelt Detection Based on the Synergy of SSM/I Data and QuikSCAT Data." *Greenstone Belts and Their Mineral Endowment* 9 (3): 955–963. doi:10.1016/j.gsf.2017.09.007.

Wei, Ting, Qing Yan, and Minghu Ding. 2019. "Distribution and Temporal Trends of Temperature Extremes Over Antarctica." *Environmental Research Letters* 14 (8): 084040. doi:10.1088/1748-9326/ab33c1.

Wille, Jonathan D., Vincent Favier, Ambroise Dufour, Irina V. Gorodetskaya, John Turner, Cécile Agosta, and Francis Codron. 2019. "West Antarctic Surface Melt Triggered by Atmospheric Rivers." *Nature Geoscience* 12 (11): 911–916. doi:10.1038/s41561-019-0460-1.

Zheng, Lei, Chunxia Zhou, Ruixi Liu, and Qizhen Sun. 2018. "Antarctic Snowmelt Detected by Diurnal Variations of AMSR-E Brightness Temperature." *Remote Sensing* 10: 9. doi:10.3390/rs10091391.

Zou, Xun, David H. Bromwich, Julien P. Nicolas, Alvaro Montenegro, and Sheng-Hung Wang. 2019. "West Antarctic Surface Melt Event of January 2016 Facilitated by Föhn Warming." *Quarterly Journal of the Royal Meteorological Society* 145 (719): 687–704. doi:10.1002/qj.3460.

Zwally, H. Jay, and Per Gloersen. 1977. "Passive Microwave Images of the Polar Regions and Research Applications." *Polar Record* 18 (116): 431–450. doi:10.1017/S0032247400000930.